Flow Maldistribution at Bubble Cap Distributor in a Plant-Scale Circulating Fluidized Bed Riser

Qingjie Guo
State Key Laboratory of Heavy Oil Processing, College of Chemistry and Chemical Engineering, University of Petroleum, Dongying, Shandong Province 257061, China

Joachim Werther, Cornelis Aue-Klett, and Ernst-Ulrich Hartge
Chemical Engineering I, Technical University Hamburg–Harburg, D-21073 Hamburg, Germany

DOI 10.1002/aic.10416
Published online March 28, 2005 in Wiley InterScience (www.interscience.wiley.com).

Flow maldistribution was investigated in an 8.5 m high circulating fluidized bed with a rectangular cross section of 1 × 0.3 m using a 14-bubble-cap distributor and a 33-bubble-cap distributor. Experimental results indicate that the bubble caps in the center region have a large flow rate and the bubble caps at the wall region have a small flow rate. The extent of the flow maldistribution is quantitatively characterized by the ratio of the maximum flow rate through a bubble cap to the average flow rate through all bubble caps (maldistribution number, V_{max}/V_{av}). A correlation is proposed for predicting flow rate distribution, maldistribution number, in the bubble cap distributor by the ratio of distributor pressure drop to riser pressure drop (pressure-drop ratio, $\Delta P_d/\Delta P_r$). © 2005 American Institute of Chemical Engineers *AIChE J,* 51: 1359–1366, 2005
Keywords: circulating fluidized bed, bubble cap, flow rate, maldistribution number, pressure-drop ratio

Introduction

In recent years, circulating fluidized beds (CFBs) have retained their leading position in developing new techniques for coal combustion, petroleum processing [fluidized catalytic cracking (FCC)], chemical reaction process, and for other industrial processes.[1,2] Consequently, there has been a growing surge of industrial and academic interest in CFBs. Unfortunately, knowledge about the minimum distributor pressure drop is relatively scarce for CFBs.[3,4] Scientists and engineers are accustomed to using rules of thumb for bubbling fluidized beds to design CFB gas distributors and to examining flow hydrodynamics in CFBs equipped with these custom-designed gas distributors. Circulating fluidized bed combustors operate at superficial gas velocities of 5–8 m/s, whereas bubbling fluidized beds operate at a superficial gas velocity of the order ≤ 1 m/s. As a consequence, there are great differences between the hydrodynamics of CFB combustors and those of bubbling fluidized beds. It is of great importance to obtain a greater knowledge of the minimum pressure drop required for an even distribution of the fluidizing gas where energy consumption for distributor pressure drop is critical. In other words, the low gas distributor pressure drop may result in a backflow of solids into the plenum chamber, whereas the large gas distributor pressure drop increases energy consumption. To introduce the background of this study, we review existing works in the literature that primarily focus on minimum pressure drop in bubbling fluidized beds.

The main function of a distributor in a fluidized bed is to guarantee a uniform distribution of gas over the whole cross-sectional area of the bed and to avoid raining of the solids and the dead space on the distributor plate.

In bubbling fluidized beds, a gas distributor results in poor fluidization if its pressure drop is too low; that is, some parts of the bed are temporarily or permanently defluidized and other parts form semipermanent spouts or channels. The desired

Correspondence concerning this article should be addressed to Q.-J. Guo at Qjguo@mail.hdpu.edu.cn.

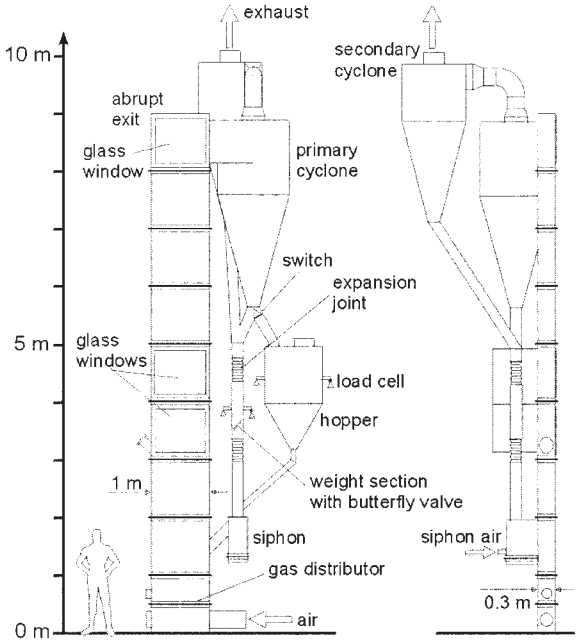

Figure 1. Pilot-plant CFB system.

properties of the distributor consist of the following: (1) uniform and stable fluidization over the entire operation range; (2) minimum attrition of bed materials; (3) minimum erosion of bed internals or heat exchanger tubes; (4) minimum backflow of solids into the plenum chamber; (5) minimum amount of dead zones on the distributor; (6) minimum plugging over extended periods of operation.

The flow behavior of distributors for bubbling fluidized beds has been investigated thoroughly by previous researchers. Thus, many guidelines for the ratio of distributor pressure drop to the bubbling bed pressure drop are available. Generally speaking, to ensure stable operation, the pressure drop across the distributor should be sufficiently large that the flow rate through it is relatively undisturbed by the bed pressure fluctuations above it. Agarwal and Davis[5] found that the distributor pressure drop should be about 10% of the bed pressure drop and never <3400 N/m^2, whereas other researchers proposed the minimum ratio of distributor to the bed pressure drop ranging from 0.02 to 0.1, with 0.3 as a widely quoted value.[6-8] Geldart[9] concluded, from the data in a two-dimensional fluidized bed, that the ratio of the bed height to bed width influenced the critical ratio c of pressure drop through distributor to bed pressure drop, as follows

$$c \geq \exp(-3.8H_{mf}/D)$$

where D is the bed diameter and H_{mf} is the bed height at the minimum fluidization condition.

Qureshi and Creasy[10] summarized the literature data on successful and unsuccessful commercial bubbling fluidized beds and introduced an aspect ratio correlation, that is

$$R_c = 0.01 + 0.2[1 - \exp(-0.5D/Z)]$$

Table 1. Physical Properties of Quartz Sand

Particle Density (kg/m^3)	Volume Concentration of Fixed Bed	Surface Mean Diameter (μm)	Minimum Fluidization Velocity* (m/s)	Terminal Settling Velocity* (m/s)
2600	0.55	140	0.03	0.93

*At ambient experimental conditions.

Table 2. Parameters of Bubble Caps

Parameter	Unit	Distributor A	Distributor B
Total volume	m^3/s	1.2	1.2
Number of bubble cap		14.0	33.0
Number of orifice		4.0	4.0
Outlet inside diameter, D_1	mm	126.0	84.0
Orifice diameter, D_2	mm	42.0	28.0
Inlet inside diameter, D_3	mm	82.5	54.5
Decreased cap diameter, D_4	mm	58, 35	38.5, 23
Inlet area	m^2	0.00535	0.00233
Orifice area	m^2	0.00554	0.00246
Annulus area	m^2	0.00626	0.00269

where R_c is the critical pressure-drop ratio of the gas distributor pressure drop to the bed pressure drop, D is the bed diameter, and Z is the bed depth.

Geldart[9] reviewed various factors influencing the distributor design in the bubbling fluidized beds, including the critical pressure-drop ratio, hole size, geometry and spacing, jet penetration depth, dead zones, particle sifting, attrition, and mixing.

Recently, Thorpe et al.[11] summarized three rules for maldistribution of bubbling fluidized beds: (1) the pressure-drop ratio method, that is, a specified ratio of distributor pressure drop to bed pressure drop; (2) the theory of Fakhimi and Harrison[12] with respect to a pressure balance for the gas passing through active and inactive gas injection points at the distributors; (3) the theory of Yue and Kolaczkowski,[13] a modification of the theory introduced by Fakhimi and Harrison.[12]

The object of the present study was to investigate the flow rate maldistribution across the CFB distributor by using two types of distributors. In particular, a relationship between the ratio of the maximum flow rate through one bubble cap to average flow rate through all bubble caps (V_{max}/V_{av}) and the ratio of distributor pressure drop to riser pressure drop ($\Delta P_d/\Delta P_r$) was investigated in detail.

Experimental

CFB system

Figure 1 illustrates a plant-scale circulating fluidized bed. The riser has a cross section of 0.3×1 m and a height of 8.5 m. Air from a 200-kW roots blower was fed to the windbox and distributed by bubble caps. A two-stage cyclone and a filter cleaned the off-gas, and the separated solids were returned to the riser at a height of 1 m above the distributor with an angle of 45°. A weighing section in the downcomer pipe measured the externally solid circulating rate.

The CFB riser is equipped with 16 pressure sensors to measure the pressure-drop profiles along the riser. The downcomer has five pressure sensors. A data-acquisition system was

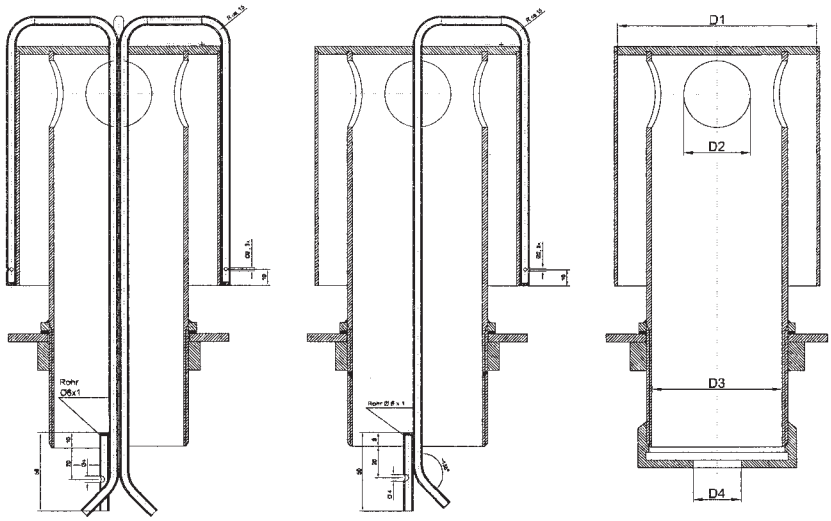

Figure 2. Cross-sectional plots of bubble in distributor.

Five measuring pipes (left), two measuring pipes (middle), no measuring pipe (right).

used for sampling data, including pressure, superficial gas velocity, sand weight in the hopper, external circulation rate, and so forth.

Quartz sand is used as the bed material and its physical properties are listed in Table 1.

Gas distributor

The design characteristics of the distributors are presented in Table 2. Two types of distributor were applied in this investigation: one has 14 bubble caps and the other has 33 bubble caps. For convenience, the 14-bubble-cap distributor is designated Distributor A and the 33-bubble-cap distributor is designated Distributor B. The 82.5 mm ID bubble caps were used in Distributor A and 54.5 mm ID bubble caps used in Distributor B. For Distributor A, two decreased caps with 58 and 35 mm ID were used to be screwed into the bubble cap for changing its flow resistance. Distributor B used 23 and 38.5 mm ID decreased caps to vary its flow resistance. Figure 2 shows various cross sections of the distributors.

Six bubble caps were used to detect the pressure drop across different bubble caps under various experimental conditions. More details of the bubble cap measurement configuration are illustrated in Figure 3. For Distributor A, bubble caps 1, 2, 4, 8, 10, and 14 were used for measurement of the pressure drops across bubble caps. Bubble caps 1, 2, 4, 10, and 14 have two pressure probes. Note that bubble cap 8 has five pressure pipes with four low-pressure measuring pipes welded along the annulus wall and the high-pressure measuring pipe fixed in the low-pressure measuring pipes, as shown in Figure 2. The pressure drop of bubble cap 8 is the average of four individual pressure drops. For Distributor B, bubble caps 12, 13, 15, 17, 20, and 22, located in the middle row, were used to determine the pressure drop across bubble caps. There were five measurement pipes for bubble cap 17. To investigate the influence of positions of measurement bubble caps on the flow rate distribution, six measurement bubble caps in Distributor B were replicated from the middle row to the border row, where their new positions were 1, 2, 4, 6, 9, and 11. With respect to CFB distributor pressure drop measurement, the high-pressure port is located at 0.18 m above the distributor, whereas the low-pressure port is connected with the wind box.

The bubble cap entrance areas (ID in mm) of 82.5, 58, 35, 54.5, 38.5, and 23 are designated as A_{a1}, A_{a2}, A_{a3}, A_{b1}, A_{b2}, and A_{b3}, respectively. As shown in Table 3, the ratio of A_{a2} to A_{a1} (Distributor A) is the same as that of A_{b2} to A_{b1} (Distributor B); also, the ratio of the A_{a3} to A_{a1} (Distributor A) is nearly equal to that of A_{b3} to A_{b1} (Distributor B).

Pressure measurement system for the bubble caps

A pressure signal system for the bubble caps is composed of 26 differential sensors, an A/D, and a computer. Low-pressure measurement and high-pressure drop measurement were attained by nine SenSym 142SC01D pressure transducers and nine SenSym 143PC5D pressure transducers, respectively. During all the experiments, nine pressure signals were simultaneously recorded at a frequency of 100 Hz for 40 s.

Results and Discussion

Pressure drop for bubble caps

Table 2 shows that the entrance area of a bubble cap is the smallest among the area of bubble cap entrance, orifice area, and annulus area. Therefore, the drag coefficient is calculated by using Eq. 1, based on the operation conditions at the bubble cap entrance.

The pressure drop across an individual bubble cap can be expressed as

$$\Delta P_{bc} = C_d \frac{\rho_o}{2} u_{in}^2 \tag{1}$$

where C_d is the drag coefficient, u_{in} is the average velocity at the entrance of the bubble cap, and ρ_o is the gas density under operating conditions at the entrance of the bubble cap.

Figures 4 and 5 illustrate the variation of the drag coefficient

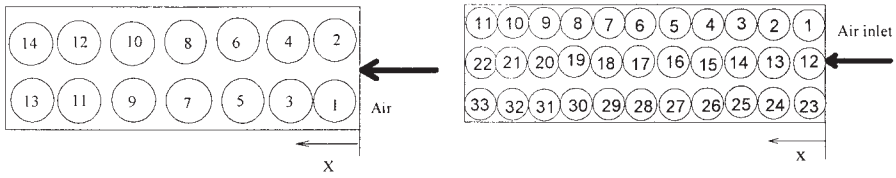

Distributor A Distributor B

Figure 3. Cross section of Distributors A and B.

Table 3. Distributor A and Distributor B Data

Distributor	Symbol of Entrance Area of a Bubble Cap	Entrance Area Ratio
A		
82.5 mm ID	A_{a1}	
58 mm ID	A_{a2}	$A_{a2}/A_{a1} = 0.494$
35 mm ID	A_{a3}	$A_{a3}/A_{a1} = 0.179$
B		
54.5 mm ID	A_{b1}	
38.5 mm ID	A_{b2}	$A_{b2}/A_{b1} = 0.494$
23 mm ID	A_{b3}	$A_{b3}/A_{b1} = 0.178$

with Reynolds number (Re_{in}) at the entrance of a bubble cap. For all decreased bubble caps, the drag coefficient is independent of Reynolds number because the Reynolds number varies at a given range.

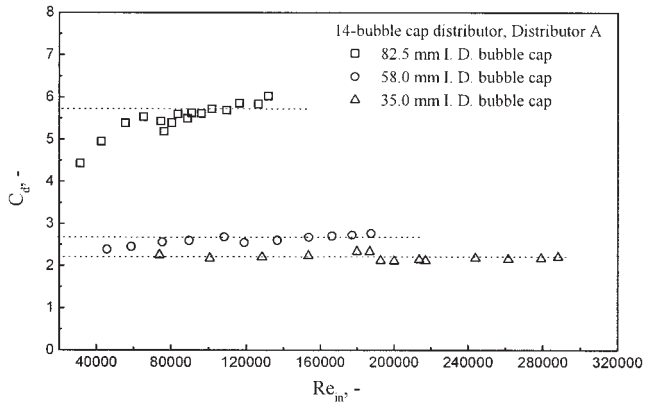

Figure 4. Effect of Reynolds number on the drag coefficient for Distributor A.

Flow rate profiles of bubble caps

Lateral flow rate profiles measured in Distributor A are shown in Figures 6 and 7. Similar profiles can be obtained at various superficial velocities and riser pressure drops. When the CFB riser is empty (that is, without particles; Figures 6a and 7a), the flow rate profiles of bubble caps exhibit a practically even flow profile, which is indicative of an almost uniform air distribution. To depict the flow rate distribution in the distributor, V_{max}/V_{min} is defined as the ratio of maximum flow rate through a bubble cap to the minimum flow rate through a bubble cap. Apparently, when the particles were added to the CFB, the flow rate profile has an uneven distribution, where $V_{max}/V_{min} = 3.53$ at a riser pressure drop of 5560 Pa. Bubble caps at the wall have small flow rates, whereas bubble caps in the center section have large flow rates. At the riser pressure drop of 7298 Pa, the ratio of V_{max}/V_{min} is reduced to 2.32. For a 35.0 mm ID bubble cap (Figure 7b), a more uniform distribution of flow rate is found. Figure 7b also illustrates the flow rate profiles where values of V_{max}/V_{min} are 1.097, 1.1, and 1.17 at riser pressure drops of 4337, 5178, and 7237 Pa, respectively, which confirms that the riser pressure drop has only a negligible effect on V_{max}/V_{min}. A comparison of Figures 6 and 7 confirms that an increased pressure drop of the distributor promotes a more uniform flow rate distribution.

Figure 8 describes the profiles of flow rate through six bubble caps (Distributor B) by using 23, 38.5, and 54.5 mm ID bubble caps at the same riser pressure drop and superficial gas velocity. $V_{max}/V_{min} = 1.417$ at a distributor pressure drop of 1101 Pa. This ratio is decreased to 1.234 at a distributor pressure drop of 1457 Pa, and then it approaches 1.06 at a distributor pressure drop of 9432 Pa. An increase in pressure drop of the distributor results in more uniform distribution of flow rate, in agreement with the conclusions drawn from Figures 6 and 7. However, the large distributor pressure drop consumes a substantial quantity of energy.

The nonuniform lateral distribution of flow rate of various bubble caps is reinforced by the core–annulus flow structure of the CFB. Berruti and colleagues[14,15] explained the high slip velocities between gas and solid in the circulating fluidized bed by assuming that the flow domain is composed of two characteristic regions: a dilute gas–solid suspension preferentially traveling upward in the center (core) and a dense phase of particle clusters or strands flowing down in the annulus near the wall. They assume that the slip velocity in the core equals the particle terminal velocity and that the density in the annulus is equal to that at the minimum fluidization. This model assumes that solids descend along the annulus at a velocity equal to the particle terminal velocity. Obvious radial suspension density gradients have been reported with a maximum at the wall and a minimum at the center, which agrees with the core–annular approximation to the flow domain. Moreover, particle velocity and solids flux measurements across the cross section of risers are nearly radially parabolic, often with negative velocities along the riser wall. Schlichthaerle and Werther[16] used fiber-optic probes to measure radial solids concentration distribution in the CFB bottom zone. For all heights the solids concentration has its minimum value in the center of the riser, and increases toward the wall. Furthermore, Schlichthaerle and Werther[17] observed intense gas backing in the wall region of the bottom zone, which resulted from the downflow of local

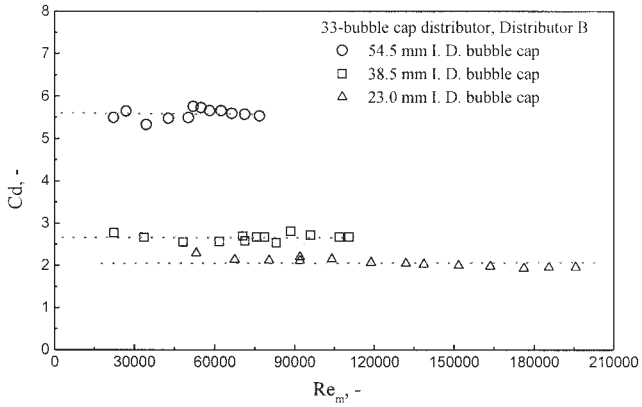

Figure 5. Effect of Reynolds number on the drag coefficient for Distributor B.

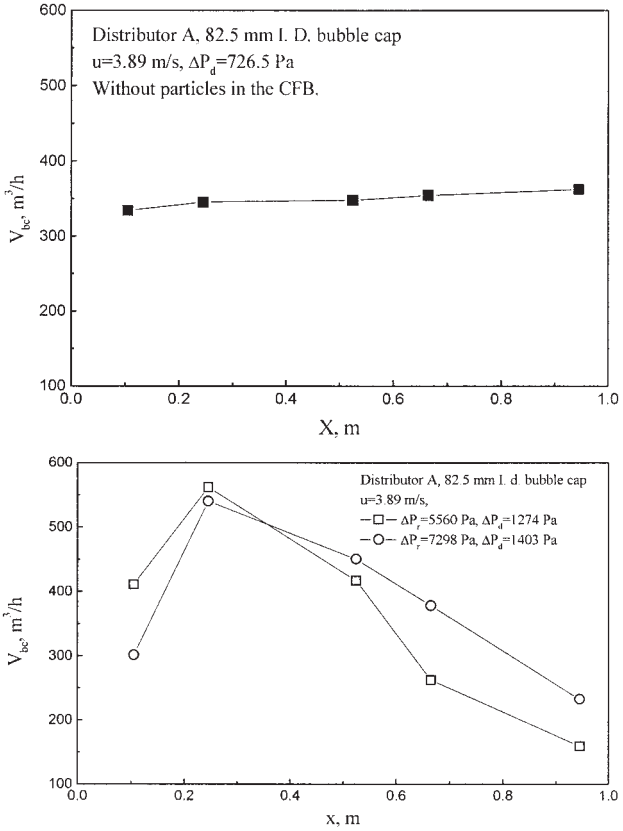

Figure 6. Lateral flow rate profiles across Distributor A with 82.5 mm ID bubble cap.

solids. Because the overall flux balance has to be fulfilled, the downward flowing solids have to change their flow direction in the bottom zone. Together, the above findings demonstrate that a core–annulus flow structure exists in the bottom zone of the CFB.

Effect of positions of measurement bubble caps on the flow rate distribution in the distributor

To investigate the influence of bubble cap positions on the flow rate distribution in the distributor, six measurement bub-

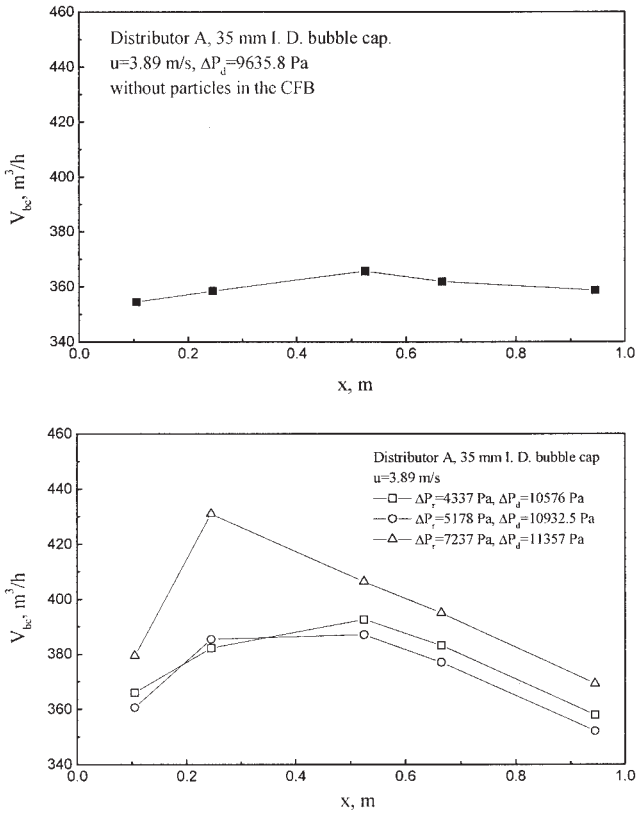

Figure 7. Lateral flow rate profiles across Distributor A with 35 mm ID bubble cap.

ble caps were replicated from the middle row to the border row. For the 54.5 mm ID bubble cap (Figure 9a), the ratios V_{max}/V_{min} in the middle row bubble caps and in the border row bubble caps are 2.60 and 3.41, respectively. As superficial gas velocity is increased to 4.5 m/s, the values of V_{max}/V_{min} in the middle row bubble caps and in the border row bubble caps are 3.43 and 2.39, respectively. There are substantial differences between V_{max}/V_{min} in the middle row bubble caps and that in the border row bubble caps as superficial gas velocity is increased from 3.0 to 4.5 m/s, suggesting that the increased pressure drop of a bubble cap resulted from increasing superficial gas velocity does not improve the maldistribution in the distributor.

When the 38.5 mm ID bubble cap was used in this test (Figure 9b), the values of V_{max}/V_{min} in the middle row bubble caps and that in the border row bubble caps reach 1.42 and 1.35 at a superficial gas velocity of 3.0 m/s. At a superficial gas velocity of 4.5 m/s, the values of V_{max}/V_{min} in the middle row bubble caps and that in the border row bubble caps are 1.20 and 1.50, respectively. It can be observed that there is still somewhat of a difference for V_{max}/V_{min} ratios between bubble caps of the middle row and those of the border row. Consequently, the increased pressure drop of a bubble cap arising from the decreasing cap entrance area (bubble cap structure parameter) improves the uniform distribution of flow rate in the distributor. In addition, there is a slight difference between the V_{max}/V_{min} ratio in the middle row bubble caps and that in the border row bubble caps.

Figure 9c highlights the uniform distribution of flow rate

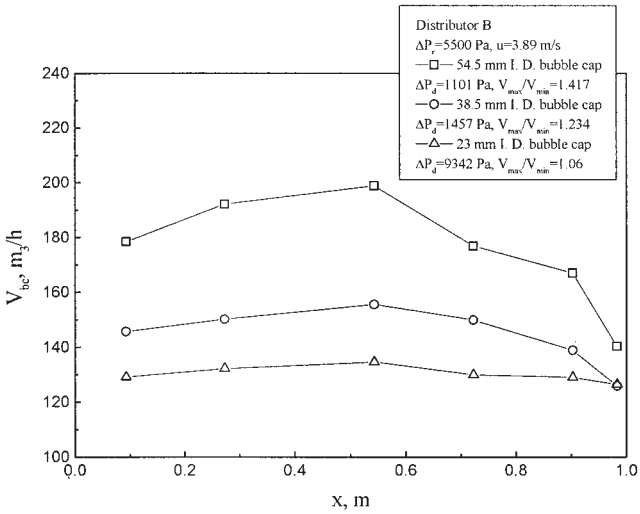

Figure 8. Profiles of flow rate of six bubble caps under a given experimental condition.

using the 23 mm ID bubble cap. In the case of 3.0 m/s, the V_{max}/V_{min} in the middle row bubble caps, 1.06, nearly approaches that in the middle row bubble caps, 1.10. Similarly, the values of V_{max}/V_{min} in the middle row bubble caps and in the border row bubble caps are nearly equal at a superficial gas velocity of 4.5 m/s. As expected, the increased pressure drops of bubble caps, resulting from the decreasing cap inlet diameter, improve the uniform distribution of flow rate in the distributor.

By comparing Figures 9a–c, one can conclude that an increase in pressure drop of the distributor results in a more uniform distribution of flow rate, which is consistent with the observations obtained from Figures 6, 7, and 8. It should be pointed out that the larger gas distributor pressure drop explains the greatly increased energy consumption.

Influence of the pressure-drop ratio $\Delta P_d/\Delta P_r$ on V_{max}/V_{min}

The pressure drop of a bubble cap is proportional to the square of its flow rate

$$\Delta P_{bc} \propto V_{bc}^2 \tag{2}$$

As discussed earlier, there is a lateral distribution for the pressure drops of various bubble caps in the distributor. That is

$$\frac{\Delta p_{\max}}{\Delta p_{\min}} = \left(\frac{V_{\max}}{V_{\min}}\right)^2 \tag{3}$$

When the superficial gas velocity varied from 3.0 to 5.2 m/s, V_{max}/V_{min} is plotted against the ratio of distributor pressure drop to riser pressure drop, $\Delta P_d/\Delta P_r$ (Figure 10). Evidently, the increased $\Delta P_d/\Delta P_r$ decreased the V_{max}/V_{min} ratio, resulting in a more uniform flow rate through different bubble caps, whereas a decreased $\Delta P_d/\Delta P_r$ only exacerbated maldistribution. Therefore, flow maldistribution can be described by $\Delta P_d/\Delta P_r$.

A comparison of Figures 6–9 indicates that the curve gradient is small in the vicinity of maximum flow rate of a bubble cap, which is easy to measure in this investigation. On the other hand, V_{min} always occurs in a part of the curve with steep gradient, which exists in the border region of a CFB. In some cases, detection of the minimum flow rate in the distributor failed because only six measurement bubble caps were used in this study. Of necessity, we used the average flow rate (V_{av}) through all bubble caps characterized by distributor maldistribution.

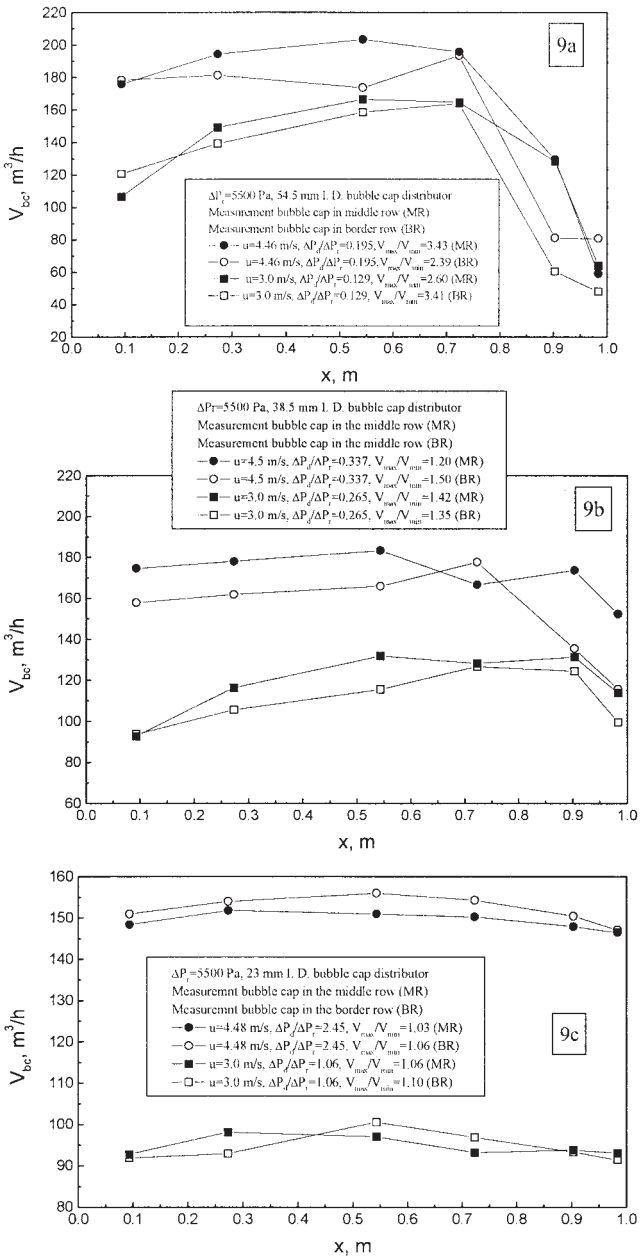

Figure 9. Effect of positions of measurement bubble caps on flow rate through different bubble caps.

MR, measurement bubble caps in middle row; BR, measurement bubble caps in border row.

Influence of the pressure-drop ratio $\Delta P_d/\Delta P_r$ on V_{min}/V_{av} and V_{max}/V_{av}

In this study, the ratio of maximum flow rate to average flow rate is defined as the maldistribution number. Figure 11 shows

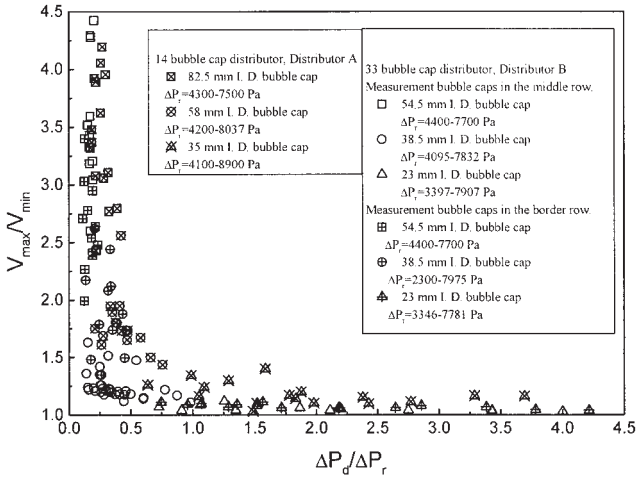

Figure 10. Influence of pressure-drop ratio on the V_{max}/V_{min} in Distributors A and B.

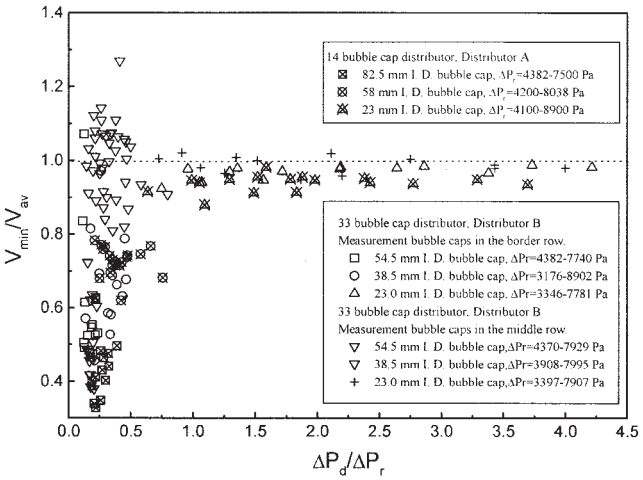

Figure 11. Influence of the pressure-drop ratio on the on V_{av}/V_{min} in Distributors A and B.

the V_{min}/V_{av} plots in Distributors A and B, where one observes that experimental data are scattered in the V_{min}/V_{av} plot characterized by a scatter distribution. It is surprising to observe that the values of many points exceed 1, demonstrating that the minimum flow rate can miss measurement under some experimental conditions. The above findings indicate that the minimum flow rate occurs frequently in the bubble caps located in the border region. Based on the above analysis, it is reasonable to use the maldistribution number (V_{max}/V_{av}) to describe maldistribution in the distributor. Figure 12 shows the effect of the pressure-drop ratio ($\Delta P_d/\Delta P_r$) on maldistribution number in Distributors A and B. A correlation with respect to the maldistribution number is expressed as

$$\frac{V_{max}}{V_{av}} = 0.903 \exp\{0.285/[(\Delta P_d/\Delta P_r) + 0.427]\} \qquad (4)$$

One should be cautious if Eq. 4 is applied in other cases beyond the present experimental conditions.

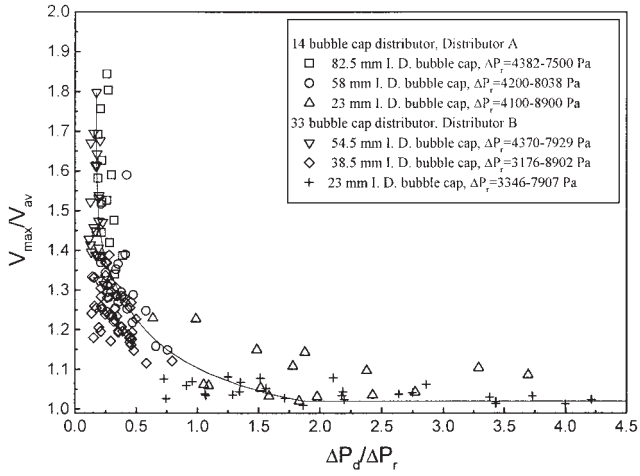

Figure 12. Influence of the pressure-drop ratio on the V_{max}/V_{av} in Distributors A and B.

From Figure 12, the maximum flow rate is about 10% higher than the average flow rate, $V_{max}/V_{av} = 1.1$, at $\Delta P_d/\Delta P_r > 1$. Furthermore, V_{max}/V_{av} tends to approach 1.2 because $\Delta P_d/\Delta P_r$ is preferentially 0.5. The maximum flow rate is 30% above the average flow rate when the ratio of distributor to bed pressure drop is 0.3, which is always the cited value for achieving a good flow rate distribution in bubbling fluidized beds. Severe maldistribution occurs with V_{max}/V_{av} varying in the range 1.2 to 1.85 if the pressure-drop ratio is <0.25. It is concluded that, to reach uniform distribution of flow rate, the pressure-drop ratio in a circulating fluidized bed ($\Delta P_d/\Delta P_r \geq 2$) is larger than that in a bubbling fluidized bed. Care is needed in extending the above conclusions to industrial CFB boilers, which calls for further investigative efforts.

Conclusions

A large number of measurements were conducted in a plant circulating fluidized bed to investigate the flow maldistribution through various bubble caps. Experimental results illustrate bubble caps at the wall have small flow rates, whereas bubble caps in the center region have larger flow rates. The increasing pressure drop of the distributor improves flow maldistribution across different bubble caps in the distributor. The extent of flow maldistribution is quantitatively characterized by the ratio of V_{max}/V_{av}, the maldistribution number. A correlation is developed for prediction of a flow rate maldistribution in the bubble cap distributor by the pressure-drop ratio $\Delta P_d/\Delta P_r$.

Acknowledgments

Dr. Qingjie Guo acknowledges a fellowship awarded by the Alexander von Humboldt Foundation. The help from Heiko Rohde, Bernhard Schult, and Sylvia Budinger during the experiments is greatly appreciated. The partial financial support of Natural Science Foundation of Shandong Province (Contract No. Z2003B01) is also acknowledged.

Notation

C_d = drag coefficient
Re_{in} = Reynolds number at the entrance of a bubble cap
u = superficial gas velocity, m/s
u_{in} = gas velocity at the entrance of a bubble cap, m/s

V_{bc} = flow rate through a bubble cap, m^3
$V_{max/Vav}$ = maldistribution number
$V_{max/Vmin}$ = ratio of maximum flow rate through a bubble cap to minimum flow rate through a bubble cap
x = horizontal coordinate (definition in Figure 3), m
ρ_o = gas density, kg/m^3
ΔP_{bc} = pressure drop through a bubble cap, Pa
ΔP_{max} = maximum pressure drop of all measurement bubble caps, Pa
ΔP_{min} = minimum pressure drop of all measurement bubble caps, Pa
ΔP_d = distributor pressure drop, Pa
ΔP_r = riser pressure drop, Pa
$\Delta P_{d/\Delta Pr}$ = pressure-drop ratio

Literature Cited

1. Werther J. Fluid mechanics of large-scale CFB units. In: Avidan AA, ed. *Circulating Fluidized Bed Technology IV*. New York, NY: American Institute of Chemical Engineers; 1994:1-16.
2. Grace JR, Avidan AA, Knowlton TM. *Circulating Fluidized Beds*. London: Blackie Academic & Professional; 1997.
3. Hartge EU, Werther J. Gas distributors for circulating fluidized bed combustors. In: Fan LS, Knowlton TM, eds. *Fluidization IX*. New York, NY: Engineering Foundation; 1998:213-210.
4. Guo QJ, Werther J. Flow behaviors in a circulating fluidized bed with various bubble-cap distributors. *Ind Eng Chem Res*. 2004;43:1756-1764.
5. Agarwal JC, Davis WL. Recent advances in blast-furnace technology. *Chem Eng Prog Symp Ser*. 1962;59:109-117.
6. Whitehead AB, Gartside G, Dent DC. Flow and pressure maldistribution at the distributor level of a gas-solid fluidized bed. *Chem Eng J*. 1970;1:175-181.
7. Davidson JF, Harrison D. *Fluidization*. London: Academic Press; 1971.
8. Perry RH, Green DW, Maloney JO. *Chemical Engineers' Handbook*. 7th ed. New York, NY: McGraw-Hill; 1997.
9. Geldart D. The design of distributor for gas-fluidized beds. *Powder Technol*. 1985;42:67-78.
10. Qureshi AE, Creasy DE. Fluidized beds gas distributors. *Powder Technol*. 1979;22:113-119.
11. Thorpe RB, Davidson JF, Pollitt M, Smith J. Maldistribution in fluidized beds. *Ind Eng Chem Res*. 2002;41:5878-5889.
12. Fakhimi S, Harrison D. Multi-orifice distributors in fluidized beds: A guide to design. Chemeca'70. Butterworth, Australia; 1970:29-36.
13. Yue PL, Kolaczkowski JA. Multiorifice distributor design for fluidized beds. *Trans IChemE*. 1982;60:164-170.
14. Berruti F, Kalogerakis N. Modeling the internal flow structure of circulating fluidized beds. *Can J Chem Eng*. 1989;68:1010-1014.
15. Berruti F, Chaoouki J, Godfroy L, Pugsley TS, Patience GS. Hydrodynamics of circulating fluidized bed risers: A review. *Can J Chem Eng*. 1995;73:579-602.
16. Schlichthaerle L, Werther J. Solids mixing in the bottom zone of a circulating fluidized bed. *Powder Technol*. 2001;120:21-33.
17. Schlichthaerle P, Werther J. Axial pressure profiles and solids concentration distributions in the CFB bottom zone. *Chem Eng Sci*. 1999;54:5485-5493.

Manuscript received Apr. 4, 2004, and revision received Sept. 27, 2004.